6-Gingerdiols as the Major Metabolites of 6-Gingerol in Cancer Cells and in Mice and Their Cytotoxic Effects on Human Cancer Cells

Lishuang Lv,[†,‡,▽] Huadong Chen,[‡,▽] Dominique Soroka,[‡] Xiaoxin Chen,[§] TinChung Leung,[#] and Shengmin Sang[‡,*]

[†]Department of Food Science and Technology, Ginling College, Nanjing Normal University, 122# Ninghai Road, Nanjing, 210097, P. R. China

[‡]Center for Excellence in Post-Harvest Technologies, North Carolina Research Campus, North Carolina Agricultural and Technical State University, 500 Laureate Way, Kannapolis, North Carolina 28081, United States

[§]Cancer Research Program, Julius L. Chambers Biomedical/Biotechnology Research Institute, North Carolina Central University, 700 George Street, Durham, North Carolina 27707, United States

[#]Nutrition Research Program, Julius L. Chambers Biomedical/Biotechnology Research Institute, North Carolina Research Campus, North Carolina Central University, 500 Laureate Way, Kannapolis, North Carolina 28081, United States

ABSTRACT: 6-Gingerol, a major pungent component of ginger (*Zingiber officinale* Roscoe, Zingiberaceae), has been reported to have antitumor activities. However, the metabolic fate of 6-gingerol and the contribution of its metabolites to the observed activities are still unclear. In the present study, we investigated the biotransformation of 6-gingerol in different cancer cells and in mice, purified and identified the major metabolites from human lung cancer cells, and determined the effects of the major metabolites on the proliferation of human cancer cells. Our results show that 6-gingerol is extensively metabolized in H-1299 human lung cancer cells, CL-13 mouse lung cancer cells, HCT-116 and HT-29 human colon cancer cells, and in mice. The two major metabolites in H-1299 cells were purified and identified as (3R,5S)-6-gingerdiol (M1) and (3S,5S)-6-gingerdiol (M2) based on the analysis of their 1D and 2D NMR data. Both metabolites induced cytotoxicity in cancer cells after 24 h, with M1 having a comparable effect to 6-gingerol in H-1299 cells.

KEYWORDS: *Ginger, 6-Gingerol, 6-Gingerdiol, Metabolite, Cancer*

INTRODUCTION

Ginger (*Zingiber officinale* Rosoce, Zingiberaceae), the fresh or processed rhizome, has been used worldwide not only as food but also as a useful crude drug in traditional Chinese medicine. With many claims of its therapeutic benefits, it has been suggested particularly for the treatment of symptoms such as inflammation, sprains, muscular aches, cramps, constipation, hypertension, fever, infectious diseases and helminthiasis, as well as rheumatic and gastrointestinal final symptoms, since antiquity.[1] The fresh rhizome of ginger contains a rich source of biologically active constituents including the main pungent principles, gingerols, with 6-gingerol be the most abundant one. Gingerols, 6-gingerol in particular, have been found to possess a variety of beneficial pharmacological effects. It has been reported that 6-gingerol treatment significantly and dose-dependently restored renal functions, reduced lipid peroxidation, and enhanced the levels of reduced glutathione and activities of superoxide dismutase and catalase against cisplatin-induced oxidative stress and renal dysfunction in rats.[2] Along with our collaborators, we have found that 6-gingerol was more effective than curcumin, a known cancer preventive agent from *Curcuma longa* L., in inhibiting 12-O-tetradecanoylphorbol 13-acetate (TPA)-induced tumor promotion in mice.[3] Pretreatment with 6-gingerol (2.5 μmol) reduced the number of tumors per mouse by 70.6% after 20-week treatment. Kim and co-workers found that 6-gingerol inhibited the proliferation and tube formation of primary cultured human endothelial cells in response to vascular endothelial growth factor (VEGF), caused cell cycle arrest in the G1 phase, and suppressed experimental metastases in tumor-bearing mice.[4] A more recent study reported that administration of 6-gingerol greatly enhanced the number of tumor-infiltrating lymphocytes in murine tumors.[5]

The pharmacokinetics of 6-gingerol in mice, rats, and humans have been examined by different research groups.[6−10] However, the metabolic fate of 6-gingerol, especially in cancer cells and in mice, is still unclear. Nakazawa and co-workers orally administrated 6-gingerol to rats and found that it could be converted to one major metabolite, 6-gingerol-4′-O-β-glucuronide, in bile and six other minor metabolites in urine.[11] It has been reported that incubation of 6-gingerol with NADPH-fortified rat hepatic microsomes gave rise to eight metabolites,[12] six of which were obtained when 6-gingerol was biotransformed by *Aspergillus niger* for one week.[13]

Despite several studies revealing some of the metabolites of 6-gingerol in microorganisms and in rats, no information is available on the metabolic fate of 6-gingerol in the cancer cells or in mice. Thus, here we report for the first time, that 6-gingerol is found to undergo metabolism in several cancer cell lines and in mice. We uniquely isolated (3R,5S)-6-gingerdiol and (3S,5S)-6-

gingerdiol as the major metabolites of 6-gingerol in cancer cells and in mice. The cytotoxicity of the two metabolites in human cancer cells was also investigated in this study.

■ MATERIALS AND METHODS

Materials. 6-Gingerol was purified from ginger extract in our laboratory.[14] Sephadex LH-20 and analytical and preparative TLC plates (250 and 2000 μm thickness, 2−25 μm particle size), dimethyl sulfoxide (DMSO), CD$_3$OD, and 3-(4,5-dimethylthiazol-2-yl)-2,5-diphenyl tetrazolium bromide (MTT) were purchased from Sigma (St. Louis, MO). HPLC-grade solvents and other reagents were obtained from VWR Scientific (South Plainfield, NJ). HPLC-grade water was prepared using a Millipore Milli-Q purification system (Bedford, MA). H-1299 human lung cancer cells, CL-13 mouse lung cancer cells, HCT-116 human colon adenocarcinoma cells, and HT-29 human colon cancer cells were obtained from American Type Tissue Culture (Manassas, VA). McCoy's 5A medium was purchased from Mediatech Inc. (Manassas, VA).

HPLC Analysis. An HPLC-ECD (ESA, Chelmsford, MA) consisting of an ESA model 584 HPLC pump, an ESA model 542 autosampler, an ESA organizer, and an ESA Coularray detector coupled with two ESA model 6210 four sensor cells was used in our study. A Gemini C18 column (150 × 4.6 mm, 5 μm; Phenomenex, Torrance, CA) was used for chromatographic analysis at a flow rate of 1.0 mL/min. The mobile phases consisted of solvent A (30 mM sodium phosphate buffer containing 1.75% acetonitrile and 0.125% tetrahydrofuran, pH 3.35) and solvent B (15 mM sodium phosphate buffer containing 58.5% acetonitrile and 12.5% tetrahydrofuran, pH 3.45). The gradient elution had the following profile: 10−30% B from 0 to 5 min; 30−55% B from 5 to 12 min; 55−100% B from 12 to 40 min; 100% B from 40 to 45 min; and 20% B from 45.1 to 55 min. The cells were then cleaned at a potential of 1000 mV for 1 min. The injection volume of the sample was 10 μL.

Biotransformation of 6-Gingerol in Cancer Cells. Cells (1.0 × 10^6) were plated in 6-well plates and allowed to attach for 24 h at 37 °C. 6-Gingerol (in DMSO) was added to McCoy's 5A medium (containing 10% fetal bovine serum, 1% penicillin/streptomycin, and 1% glutamine) to reach a final concentration of 10 μM and then incubated with different cancer cells. At several time points (0, 30 min, 1, 2, 4, 6, 8, and 24 h), 190 μL samples were taken, and transferred to vials containing 10 μL of 0.2% ascorbic acid to stabilize 6-gingerol and its metabolites. Metabolism was halted and metabolites were extracted with acetonitrile. Samples were immediately analyzed or stored at −80 °C before HPLC analysis.

Purification of the Major Metabolites of 6-gingerol in H-1299 Cells. 6-Gingerol (200 μM) was incubated with H-1299 cells for 48 h at 37 °C. The cell culture medium (total 1.0 L) was then extracted with ethyl acetate (3 times, each time 1.0 L). The ethyl acetate residue was dissolved in ethanol and underwent chromatography on a Sephadex LH-20 column with 95% ethanol as eluent to remove the background components in the cell culture medium and to generate 6-gingerol and its metabolites in an enriched fraction. This fraction was further purified by preparative TLC (hexane−acetone, 7:3, v/v) to afford 5.1 mg M1 and 5.2 mg M2 (Figure 1).

Nuclear Magnetic Resonance (NMR) Analysis. ^{1}H, ^{13}C, and two-dimensional (2-D) spectra were acquired on a Bucker AVANCE 700 MHz instrument (Bruker, Inc., Silberstreifen, Rheinstetten, Germany). All compounds were analyzed in CD$_3$OD. ^{1}H and ^{13}C NMR data of M1 and M2 are listed in Table 1.

Treatment of Mice and Urine Sample Collection. Experiments with mice were carried out according to a protocol approved by the Institutional Review Board for the Animal Care and Facilities Committee at North Carolina Central University. Female C57BL/6J mice were purchased from the Jackson Laboratory (Bar Harbor, ME) and allowed to acclimate for at least 1 week prior to the start of the experiment. The mice were housed 5 per cage and maintained in air-conditioned quarters with a room temperature of 20 ± 2 °C, relative humidity of 50 ± 10%, and an alternating 12 h light/dark cycle. Mice were fed Purina Rodent Chow #5001 (Research Diets) and water, and were allowed to eat and drink ad libitum. 6-Gingerol in corn oil was
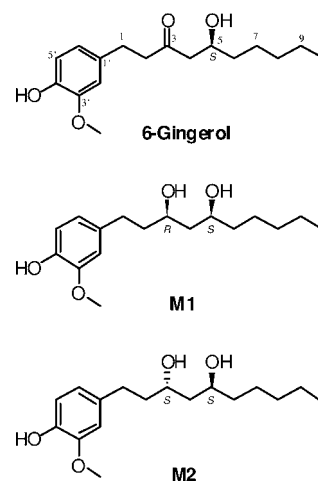

Figure 1. Chemical structures of 6-gingerol and its major metabolites M1 and M2.

Table 1. δ_H (700 MHz) and δ_C (175 MHz) NMR Spectra Data of M1 and M2 (CD$_3$OD, δ in ppm and J in Hz)

	M1		M2	
	δ_C	δ_H multi (J)	δ_C	δ_H multi (J)
1′	133.9 s		133.87 s	
2′	110.97 d	6.85 d (7.9)	110.90 d	6.82 d (8.0)
3′	146.41 s		146.39 s	
4′	143.68 s		143.68 s	
5′	114.24 d	6.74 d (1.8)	114.23 d	6.69
6′	120.89 d	6.71 d (7.9, 1.8)	120.83 d	6.64 d (7.9, 1.5)
1	31.80 t	2.64 m	33.12 t	2.61 m
		2.73 m		2.72 m
2	40.06 t	1.78 m	39.39 t	1.84 m
		1.81 m		
3	72.41 d	3.89 m	69.57 d	3.96 m
4	42.94 t	1.64 m	42.37 t	1.65 m
5	73.40 d	3.84 m	68.95 d	3.91 m
6	38.35 t	1.45 m	37.48 t	1.46 m
7	25.03 t	1.30 m	25.42 t	1.30 m
8	31.44 t	1.30 m	31.78 t	1.30 m
9	22.64 t	1.30 m	22.59 t	1.30 m
10	14.07 q	0.91 t (7.2)	14.02 q	0.89 t (7.2)
1″	55.87 q	3.87 s	55.85 q	3.87 s

administered to mice by oral gavage (200 mg/kg). Urine samples were collected in metabolism cages (5 mice per cage) for 24 h after administration of vehicle (control group, n = 5) or 6-gingerol (treated group, n = 5). Samples were stored at −80 °C before analysis.

Urine Sample Preparation. For conjugated metabolites, 950 μL methanol was added to each urine sample (50 μL from control and 6-gingerol-treated group, respectively) to precipitate proteins. After centrifugation at 17 × 1000 rpm for 5 min, the supernatant was transferred into vials for HPLC-ECD and LC/MS analysis. Enzymatic deconjugation was performed as described previously with slight modification.[15] In brief, duplicate samples were prepared in the presence of β-glucuronidase (250 U) and sulfatase (3 U) for 24 h at 37 °C and then extracted twice with ethyl acetate. The ethyl acetate fraction was dried under vacuum, and the solid was resuspended in 200 μL of 80% aqueous methanol with 0.1% acetic acid for further HPLC-ECD and LC/MS analysis.

LC/ESI-MS Method. LC/MS analysis was carried out with a Thermo-Finnigan Spectra System which consisted of an Accela high-speed MS pump, an Accela refrigerated autosampler, and an LCQ Fleet ion trap mass detector (Thermo Electron, San Jose, CA) incorporated
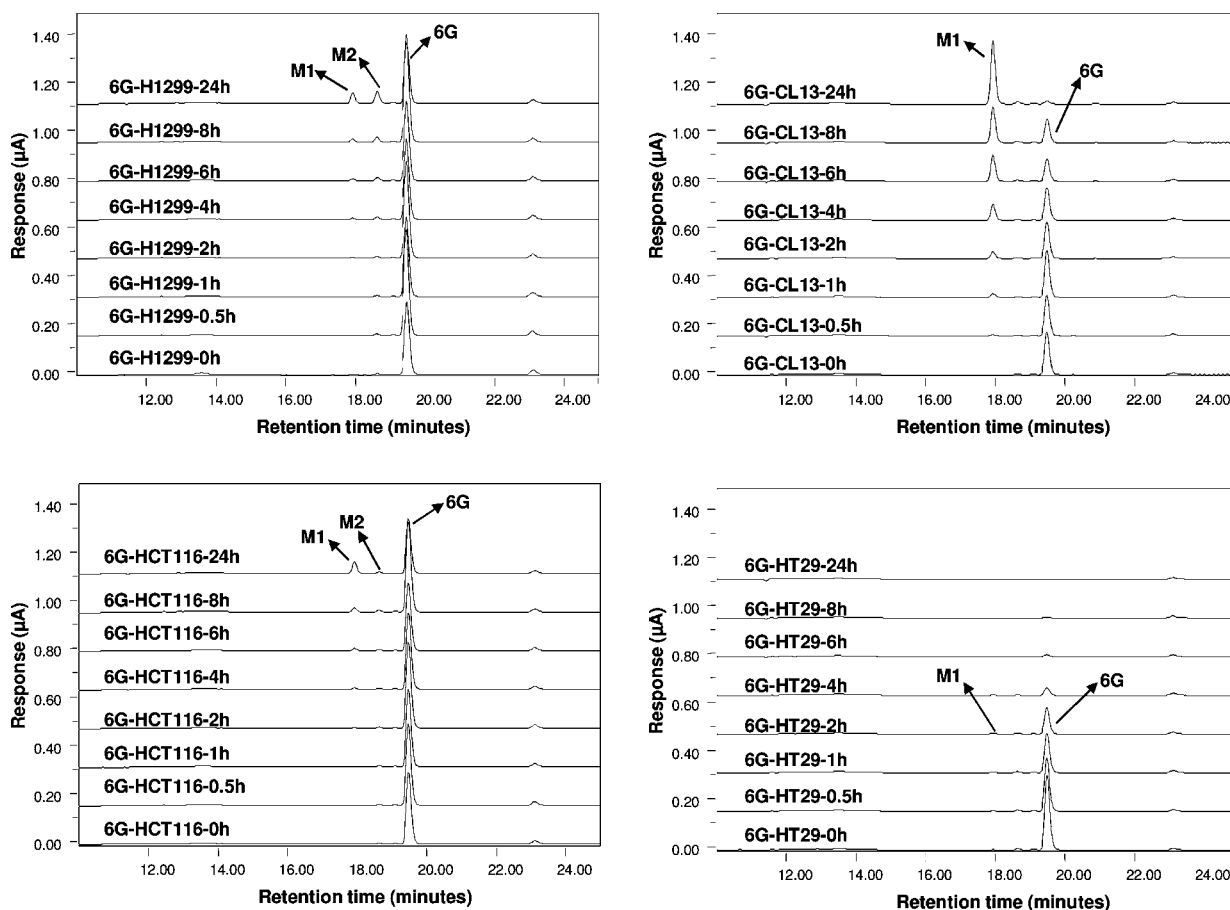
11373

dx.doi.org/10.1021/jf303879b | *J. Agric. Food Chem.* 2012, 60, 11372−11377

Figure 2. HPLC-ECD chromatograms of cultured media of 6-gingerol treated H-1299, CL-13, HCT-116, and HT-29 cell lines.

with electrospray ionization (ESI) interfaces. A Luna C18 column (50 × 2.0 mm i.d., 3 μm; Phenomenex, Torrance, CA) was used for separation at a flow rate of 0.2 mL/min. The column was eluted with 100% solvent A (5% aqueous methanol with 0.2% acetic acid) for 2 min, followed by linear increases in B (95% aqueous methanol with 0.2% acetic acid) to 45% from 2 to 15 min, to 85% from 15 to 45 min, to 100% from 45 to 50 min, and then with 100% B from 50 to 55 min. The column was then re-equilibrated with 100% A for 5 min. The LC eluent was introduced into the ESI interface. The positive and negative ion polarity mode was set for the ESI source with the voltage on the ESI interface maintained at approximately 4.5 kV. Nitrogen gas was used as the sheath gas at a flow rate of 30 units and the auxiliary gas at 5 units. Optimized parameters included ESI capillary temperature, capillary voltage, ion spray voltage, sheath gas flow rate, tube lens offset voltage, and ion optics settings. These parameters were tuned by a 6-gingerol standard. The collision-induced dissociation (CID) was conducted with an isolation width of 2 Da and normalized collision energy of 35 for both MS^2 and MS^3. Default automated gain control target ion values were used for MS, MS^2, and MS^3 analyses. The mass range was measured from 50 to 1000 m/z. Data acquisition was performed with Xcalibur 2.0 version (Thermo Electron, San Jose, CA, USA).

Growth Inhibition against Human Lung and Colon Cancer Cells. Cell growth inhibition was determined by (4,5-dimethylthiazol-2-yl)-2,5-diphenyltetrazolium bromide (MTT) colorimetric assay MTT assays.[16] Cells (1.5 × 10^4) were plated in 96-well microtiter plates and allowed to attach for 24 h at 37 °C. The test compounds (in DMSO) were added to cell culture medium to desired final concentrations (final DMSO concentrations for control and treatments were 0.1%). After culturing for 24 h, the medium was aspirated, and the cells were treated with 100 μL fresh medium containing 2.41 mmol/L MTT. Following incubation for 3 h at 37 °C, the MTT-containing medium was aspirated, 100 μL DMSO was added to solubilize the formazan precipitate, and the plate was read at 570 nm on a microtiter plate reader. The reading

reflected the number of viable cells, and was expressed as % viable cells in control. Both H-1299 and HCT-116 cells were cultured in McCoy's 5A medium. All the above media were supplemented with 10% fetal bovine serum, 1% penicillin/streptomycin, and 1% glutamine, and the cells were kept in a 37 °C incubator with 95% humidity and 5% CO$_2$.

■ RESULTS AND DISCUSSION

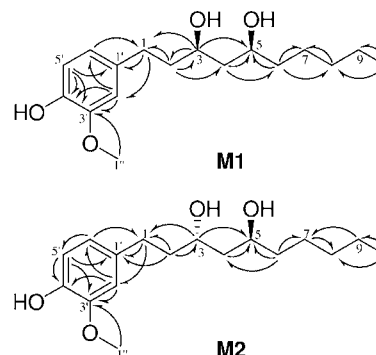**Biotransformation of 6-Gingerol in H-1299, CL-13, HCT-116, and HT-29 Cancer Cells.** We found that 6-gingerol

Figure 3. Significant HMBC (H → C) correlations of M1 and M2.

is very stable in culture media (data not shown). After incubation of 6-gingerol with four different cancer cell lines (H-1299, CL-13, HCT-116, and HT-29), the culture media were collected at several time points and analyzed by HPLC with electrochemical detection. Our results show that 6-gingerol was extensively
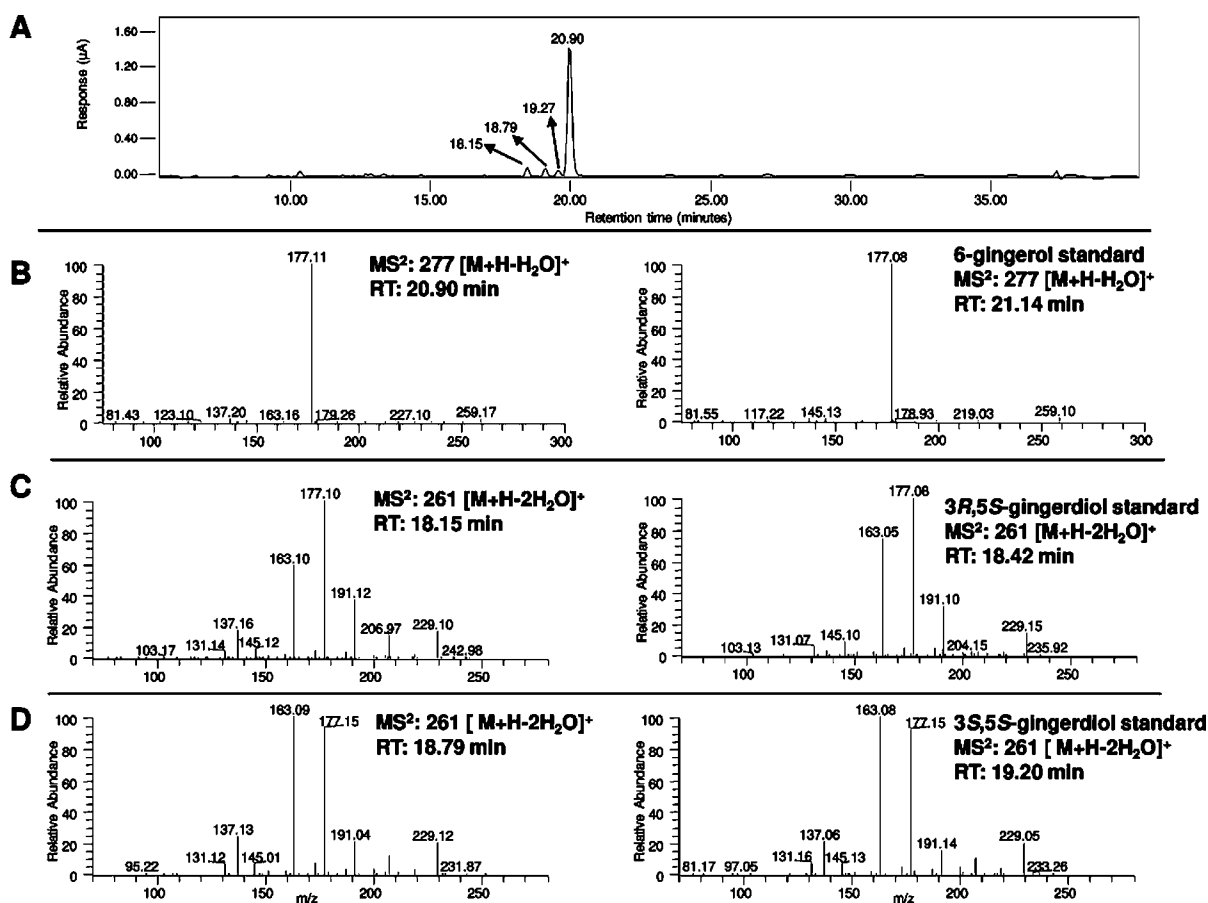
Figure 4. (A) HPLC chromatogram of the urinary sample after hydrolysis with sulfatase and glucuronidase collected from 6-gingerol treated mice; (B-D) MS^2 (positive ion) spectra of peaks at 20.90, 18.15, and 18.79 min in the enzymatic deconjugated mouse urine samples and MS^2 (positive ion) spectra of authentic 6-gingerol, (3R,5S)-6-gingerdiol, and (3S,5S)-6-gingerdiol.

metabolized in all four cancer cell lines (Figure 2). After 24 h incubation, two major metabolites (M1 and M2) appeared in H-1299 human lung cancer cells, M1 was observed as the major metabolite in CL-13 mouse lung cancer cells and in HCT-116 human colon cancer cells, and M2 was observed as the minor metabolite in CL-13 cancer cells. At 24 h, 6-gingerol was almost completely converted to M1 in CL-13 cells. M1 was also observed as the metabolite of 6-gingerol in HT-29 human colon cancer cells, however, both M1 and 6-gingerol were disappeared after 24 h incubation.
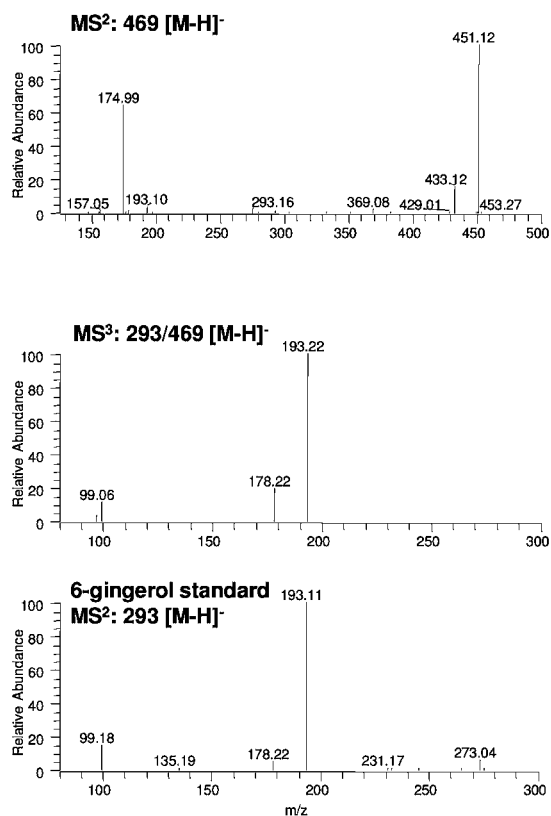
Purification and Structure Elucidation of the Metabolites of 6-Gingerol in H-1299 Human Lung Cancer Cells. After 48 h incubation of 6-gingerol with H-1299 cells, the two major metabolites were purified from the culture medium using a Sephadex LH-20 column and preparative TLC. Their structures were established by analyzing the ^{1}H, ^{13}C, and 2D NMR (HMQC and HMBC) spectra as well as by comparing with literature data.[17] Metabolite M1 showed the molecular formula $C_{17}H_{28}O_4$ based on positive ESI-MS at m/z 261 $[M + H - 2H_2O]^+$ and its ^{1}H and ^{13}C NMR data (Table 1). The molecular weight of M1 was 2 mass units higher than that of 6-gingerol, indicating that M1 might be the keto group reduced metabolite of 6-gingerol. In addition to the distinguishable resonance for an methoxyl group (δ_H 3.87, 3H, s), the ^{1}H NMR spectrum of M1 (Table 1) also indicated the presence of a 1,3,4-trisubstituted phenyl group [δ_H 6.85 (1 H, $J = 7.9$ Hz); 6.74 (1 H, d, $J = 1.8$ Hz); and 6.71 (1 H, ddd, $J = 7.9, 1.8$ Hz)] and a methyl group (δ_H 0.91, 3H, t, $J = 7.2$ Hz). Its ^{13}C NMR spectrum (Table 1) displayed 17

carbon resonances, which were classified by HMQC experiments as two methyls, seven methylenes, five methine, and three quaternary carbons. The aforementioned NMR data implied the structure of M1 was closely related to that of [6]-gingerol. The only difference was the C-3 of M1 being assigned as an oxymethine (δ_H 3.89, 1H, m; δ_C 72.41) instead of the expected ketone carbonyl in [6]-gingerol. This was confirmed by the HMBC (Figure 3) correlations of H-3/C-1, H-3/C-2, H-3/C-5 and H-2/C-3. Therefore, we confirmed that M1 is the keto reduced metabolite of 6-gingerol, 6-ginerdiol.

M2 showed the same molecular formula as M1 based on ESI-MS at m/z 261 $[M + H - 2H_2O]^+$ and its ^{1}H and ^{13}C NMR data. M2 had similar NMR spectra to those of M1. Its HMBC spectrum further confirmed that M2 possessed the same planar structure as that of M1 (Figure 3). Since a new chiral center was formed in M1 and M2, thus the difference between M1 and M2 is the configuration at C-3. After comparing the NMR data of M1 and M2 with those of the two known 6-gingerdiol, (3R,5S)-gingerdiol and (3S,5S)-gingerdiol, we confirmed that the configurations of M1 and M2 at C-3 are R and S, respectively.[17] Therefore, M1 and M2 were identified as (3R,5S)-gingerdiol and (3S,5S)-gingerdiol (Figure 1), respectively.

Biotransformation of 6-Gingerol in Mice. Urine samples collected from 6-gingerol-treated mice (200 mg/kg, *i.g.*) were analyzed. After enzymatic deconjugation, the HPLC chromatography (Figure 4A) showed four peaks. The peaks at 18.15, 18.79, and 20.90 min were identified as M1, M2 and 6-gingerol by comparing their MS^2 spectra with those of authentic 3R,5S-

A: ESI negative

MS^2: 469 [M-H]$^-$

MS^3: 293/469 [M-H]$^-$

6-gingerol standard
MS^2: 293 [M-H]$^-$

B: ESI positive

MS^2: 493 [M+Na]$^+$

MS^3: 317/493 [M+Na]$^+$

6-gingerol standard
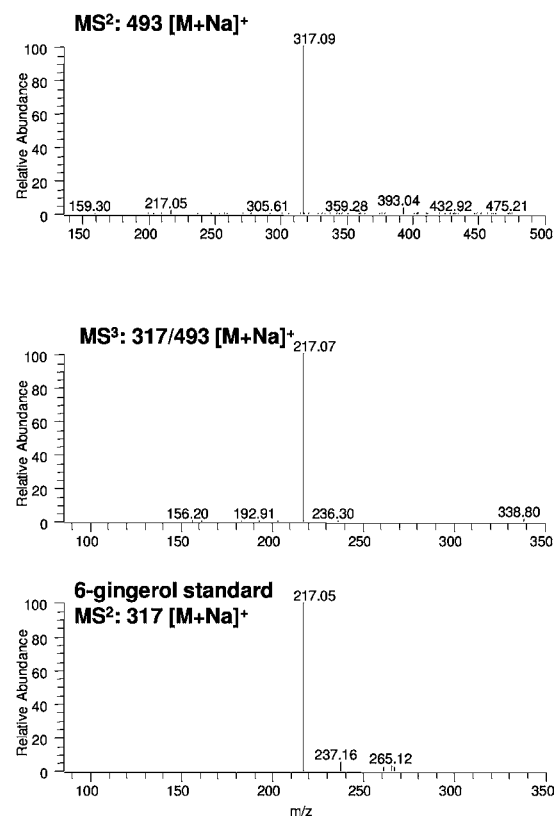### MS^2: 317 [M+Na]$^+$

Figure 5. (A) MS^2 and MS^3 (negative ion) spectra of the monoglucuronidated 6-gingerol, and MS^2 (negative ion) spectrum of authentic 6-gingerol; (B) MS^2 and MS^3 (positive ion) spectra of monoglucuronidated 6-gingerol, and MS^2 (positive ion) spectrum of authentic 6-gingerol.

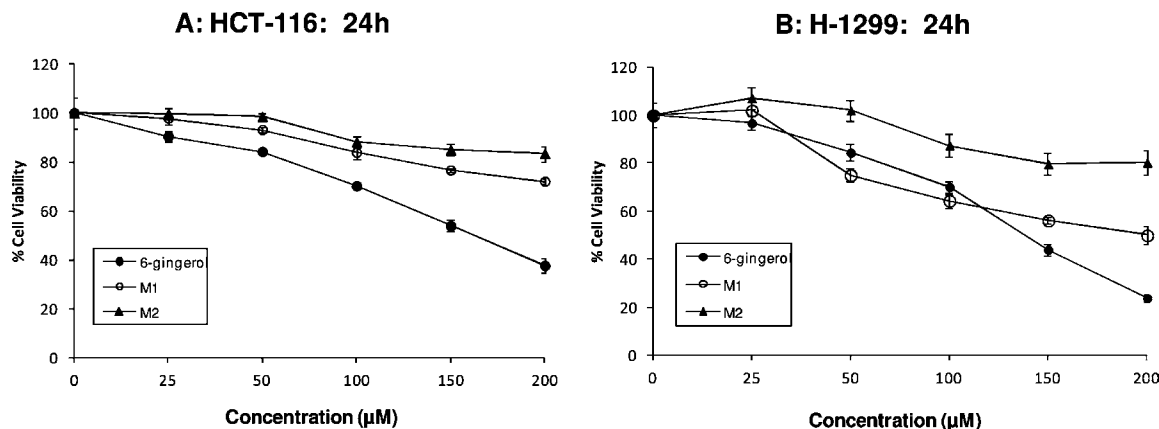## A: HCT-116: 24h

B: H-1299: 24h

Figure 6. Cytotoxicity effect of 6-gingerol and its metabolites on human cancer cells. Human colon cancer cells HCT-116 (A) and nonsmall cell lung carcinoma cell line H1299 (B) were treated with different concentration of 6-gingerol and its metabolites (M1 and M2) (0, 25, 50, 100, 150, and 200 μM) for 24 h. Cell viability was determined by the MTT assay.

gingerdiol, 3S,5S-gingerdiol, and 6-gingerol, respectively (Figure 4B−D). There was an unknown peak at 19.27 min besides M1, M2, and 6-gingerol. However, we were unable to deduce the structure of this peak based on its tandem mass spectra.

Without enzymatic deconjugation, we found that 6-gingerol, M1 and M2 were existed in their glucuronidated forms (over 95%). However, the glucuronidated metabolites of M1 and M2 had very poor ionization under both ESI negative and positive modes and we were unable to elucidate their structures using tandem mass. Under ESI negative mode, the MS^2 spectrum of the monoglucuronidated 6-gingerol (m/z 469 [M−H]$^-$) had the

product ion m/z 293 [M − 176 − H]$^-$ and the tandem mass spectrum of this product ion (MS^3: m/z 293/469) was identical to the MS^2 spectrum of authentic 6-gingerol (Figure 5A), suggesting that it is monoglucuronidated 6-gingerol. In addition, the MS^2 spectrum of the monoglucuronidated 6-gingerol had m/z 175 and 451 as its major product ions, indicating the glucuronic acid moiety was conjugated at the phenolic hydroxyl group.[12] In contrast, under ESI positive detection, the sodium adduct ion at m/z 493 [M + Na]$^+$ of the monoglucuronidated 6-gingerol was detected (Figure 5B). The MS^3 spectrum of its product ion m/z 317 [M − 176 + Na]$^+$ (MS^3: m/z 317/493) was almost identical

11376

dx.doi.org/10.1021/jf303879b | J. Agric. Food Chem. 2012, 60, 11372−11377

to the MS^2 spectrum of the sodium adduct ion of authentic 6-gingerol (m/z 317 $[M + Na]^+$) (Figure 5B).

Effects of 6-Gingerol and Its Metabolites on the Proliferation of Human Cancer Cells. We investigated the effects of 6-gingerol and its two metabolites, M1 and M2 (0, 25, 50, 100, 150, and 200 μM), on the inhibition of cell growth in HCT-116 human colon cancer cells and H-1299 human lung cancer cells. As shown in Figure 6A, 6-gingerol inhibited the growth of HCT-116 cells in a dose-dependent manner with an IC_{50} of 160.42 μM. The two metabolites, M1, and M2, also demonstrated inhibition on the growth of HCT-116 cells. Whereas their inhibitory activities ($IC_{50} > 200$ μM) were weaker than that of 6-gingerol in HCT-116 cells, in H-1299 cells, the metabolite M1 exhibited measurable growth inhibition ($IC_{50} = 200$ μM). 6-Gingerol displayed the highest potency in this cell line, with an IC_{50} of 136.73 μM after 24 h (Figure 6B).

In the present study, we investigated the metabolic profile of [6]-gingerol in cancer cells lines and in mice in order to afford a greater understanding of its mechanistic efficacy in these two models. Our findings yielded two major metabolites, (3R,5S)-6-gingerdiol and (3S,5S)-6-gingerdiol, which were then tested for in vitro activity. Both metabolites showed some cancer cell growth inhibition, albeit less activity than 6-gingerol. 6-Gingerdiols have been reported as the metabolite of 6-gingerol in rat liver microsome [12] as well as the minor components in ginger rhizome.[18] They have displayed higher potency than 6-gingerrol in other mechanistic paradigms. It has been reported that nitric oxide production in RAW264 macrophage cells was preferentially inhibited by (3R,5S)-6-gingerdiol and (3S,5S)-6-gingerdiol, with more than 70% inhibition at 100 μg/mL, while 6-gingerol gave no inhibition at this concentration.[19] Abdel-Aziz and co-workers found that 6-gingerdiol had a greater 5-HT3 receptor blocking activity than 6-gingerol in $N1 \times 10^{-115}$ cells.[20] The above evidence taken in tandem with our findings indicate that the metabolites of [6]-gingerol from human cancer cell lines and CL-13 mouse cancer cells may not exert cyotoxicity as a primary means of bioactivity but are still pharmacologically operative.

■ AUTHOR INFORMATION

Corresponding Author

*Phone: 704-250-5710. E-mail: ssang@ncat.edu.

Author Contributions

▽These authors contributed equally to this work.

Notes

The authors declare no competing financial interest.

■ REFERENCES

(1) Ali, B. H.; Blunden, G.; Tanira, M. O.; Nemmar, A. Some phytochemical, pharmacological and toxicological properties of ginger (Zingiber officinale Roscoe): Areview of recent research. *Food Chem. Toxicol.* **2008**, *46* (2), 409−20.

(2) Kuhad, A.; Tirkey, N.; Pilkhwal, S.; Chopra, K. 6-Gingerol prevents cisplatin-induced acute renal failure in rats. *Biofactors* **2006**, *26* (3), 189−200.

(3) Wu, H.; Hsieh, M. C.; Lo, C. Y.; Liu, C. B.; Sang, S.; Ho, C. T.; Pan, M. H. 6-Shogaol is more effective than 6-gingerol and curcumin in inhibiting 12-O-tetradecanoylphorbol 13-acetate-induced tumor promotion in mice. *Mol. Nutr. Food Res.* **2010**, *54* (9), 1296−306.

(4) Kim, E. C.; Min, J. K.; Kim, T. Y.; Lee, S. J.; Yang, H. O.; Han, S.; Kim, Y. M.; Kwon, Y. G. [6]-Gingerol, a pungent ingredient of ginger, inhibits angiogenesis in vitro and in vivo. *Biochem. Biophys. Res. Commun.* **2005**, *335* (2), 300−8.

(5) Ju, S. A.; Park, S. M.; Lee, Y. S.; Bae, J. H.; Yu, R.; An, W. G.; Suh, J. H.; Kim, B. S. Administration of 6-gingerol greatly enhances the number of tumor-infiltrating lymphocytes in murine tumors. *Int. J. Cancer* **2012**, *130* (11), 2618−28.

(6) Zick, S. M.; Djuric, Z.; Ruffin, M. T.; Litzinger, A. J.; Normolle, D. P.; Alrawi, S.; Feng, M. R.; Brenner, D. E. Pharmacokinetics of 6-gingerol, 8-gingerol, 10-gingerol, and 6-shogaol and conjugate metabolites in healthy human subjects. *Cancer Epidemiol., Biomarkers Prev.* **2008**, *17* (8), 1930−6.

(7) Ding, G. H.; Naora, K.; Hayashibara, M.; Katagiri, Y.; Kano, Y.; Iwamoto, K. Pharmacokinetics of [6]-gingerol after intravenous administration in rats. *Chem Pharm Bull (Tokyo)* **1991**, *39* (6), 1612−4.

(8) Jiang, S. Z.; Wang, N. S.; Mi, S. Q. Plasma pharmacokinetics and tissue distribution of [6]-gingerol in rats. *Biopharm. Drug Dispos.* **2008**, *29* (9), 529−37.

(9) Kim, M. G.; Shin, B. S.; Choi, Y.; Ryu, J. K.; Shin, S. W.; Choo, H. W.; Yoo, S. D. Determination and pharmacokinetics of [6]-gingerol in mouse plasma by liquid chromatography-tandem mass spectrometry. *Biomed. Chromatogr.* **2012**, *26* (5), 660−5.

(10) Naora, K.; Ding, G.; Hayashibara, M.; Katagiri, Y.; Kano, Y.; Iwamoto, K. Pharmacokinetics of [6]-gingerol after intravenous administration in rats with acute renal or hepatic failure. *Chem Pharm Bull (Tokyo)* **1992**, *40* (5), 1295−8.

(11) Nakazawa, T.; Ohsawa, K. Metabolism of [6]-gingerol in rats. *Life Sci.* **2002**, *70* (18), 2165−75.

(12) Pfeiffer, E.; Heuschmid, F. F.; Kranz, S.; Metzler, M. Microsomal hydroxylation and glucuronidation of [6]-gingerol. *J. Agric. Food Chem.* **2006**, *54* (23), 8769−74.

(13) Hironobu Takahashi, T. H.; Noma, Yoshiaki; Asakawa, Y. Biotransformation of 6-gingerol and 6-shogaol by Aspergillus niger. *Phytochemistry* **1993**, *34* (6), 1497−1500.

(14) Sang, S.; Hong, J.; Wu, H.; Liu, J.; Yang, C. S.; Pan, M. H.; Badmaev, V.; Ho, C. T. Increased growth inhibitory effects on human cancer cells and anti-inflammatory potency of shogaols from Zingiber officinale relative to gingerols. *J. Agric. Food Chem.* **2009**, *57* (22), 10645−50.

(15) Shao, X.; Chen, X.; Badmaev, V.; Ho, C. T.; Sang, S. Structural identification of mouse urinary metabolites of pterostilbene using liquid chromatography/tandem mass spectrometry. *Rapid Commun. Mass Spectrom.* **2010**, *24* (12), 1770−8.

(16) Momann, T. Rapid colorimetric assay for cellular growth and survival: application to proliferation and cytotoxicity assays. *J. Immunol. Methods* **1983**, *65*, 55−63.

(17) Kikuzaki, H.; Tsai, S.-M.; Nakatani, N. Gingerdiol related compounds from the rhizomes of Zingiber officinale. *Phytochemistry* **1992**, *31* (5), 1783−1786.

(18) Feng, T.; Su, J.; Ding, Z. H.; Zheng, Y. T.; Li, Y.; Leng, Y.; Liu, J. K. Chemical constituents and their bioactivities of "Tongling White Ginger" (Zingiber officinale). *J. Agric. Food Chem.* **2011**, *59* (21), 11690−5.

(19) Shimoda, H.; Shan, S. J.; Tanaka, J.; Seki, A.; Seo, J. W.; Kasajima, N.; Tamura, S.; Ke, Y.; Murakami, N. Anti-inflammatory properties of red ginger (Zingiber officinale var. Rubra) extract and suppression of nitric oxide production by its constituents. *J. Med. Food* **2010**, *13* (1), 156−62.

(20) Abdel-Aziz, H.; Nahrstedt, A.; Petereit, F.; Windeck, T.; Ploch, M.; Verspohl, E. J. 5-HT3 receptor blocking activity of arylalkanes isolated from the rhizome of Zingiber officinale. *Planta Med.* **2005**, *71* (7), 609−16.